

## Structural Studies of $\beta$ -Bi<sub>2</sub>O<sub>3</sub> Stabilized by the Addition of PbF<sub>2</sub>

S. HORIUCHI, F. IZUMI, T. MITSUHASHI, AND K. UCHIDA\*

*National Institute for Research in Inorganic Materials, Tsukuba,  
Ibaraki 305, Japan*

AND T. SHIMOMURA AND K. OGASAHARA

*Mitsubishi Gas Chemicals, Katsushika-ku, Tokyo 125, Japan*

Received June 24, 1987; in revised form November 18, 1987

Structural variations in 85% Bi<sub>2</sub>O<sub>3</sub> · 15% PbF<sub>2</sub> quenched from 800°C and then reheated at lower temperature are examined mainly by transmission electron microscopy. The quenched specimen is composed of the tetragonal  $\beta$ -phase and shows a microstructure with ill-defined bands. An incommensurate superstructure is generated to produce extra reflections, which can be indexed based on a one-dimensional modulated structure along the *c* direction. On reheating, a second phase of rhombohedral symmetry with the lattice parameters *a* = 12.0 and *c* = 37.1 Å separates from the  $\beta$ -phase. Precipitation precedes the phase separation © 1988 Academic Press, Inc.

### 1. Introduction

In a previous paper (1) we reported that addition of PbF<sub>2</sub> into Bi<sub>2</sub>O<sub>3</sub> causes stabilization of the  $\beta$ -phase (tetragonal) and a supercell three times larger in the *c* direction is formed. With further investigation we have found that the structure strongly depends on a heat treatment of specimens; the phase decomposes to produce a second one and the matrix remarkably changes the lattice parameters. The present paper aims to describe the structural variation during the heat treatment as examined primarily by means of transmission electron microscopy.

### 2. Experimental Procedure

The powder of  $\beta$ -PbF<sub>2</sub> (purity, 99.9%) was mixed together with that of  $\alpha$ -Bi<sub>2</sub>O<sub>3</sub> (purity, 99.9%) with a molar ratio of 15/85. The mixed powders were heated at 800°C for 5 hr in sealed Pt capsules and then quenched in water to room temperature. X-ray powder diffraction using a diffractometer (Rigaku conventional type) showed that the product was composed of a single phase. Some of the quenched products were reheated in sealed capsules at 400 and 250°C. It was noted that a second phase appeared in the specimen.

Small blocks of products were ground in an agate mortar. The fragments obtained were mounted on carbon microgrids and examined in a 1-MV electron microscope (Hitachi-1250 type). Additionally a differ-

\* Presently with Ube Kosan Co.

TABLE I  
LATTICE SPACING ( $d$ ) AND THE INTENSITY ( $I$ )  
OBTAINED BY X-RAY POWDER DIFFRACTION FOR  
THE SPECIMENS

Specimen A		$\beta$ -Phase <sup>a</sup>		Specimen B		$\beta$ -Phase <sup>b</sup>		Second phase	
$d_{\text{obs}}$ (Å)	$I_{\text{obs}}$	$d_{\text{cal}}$ (Å)	$hkl$	$d_{\text{obs}}$ (Å)	$I_{\text{obs}}$	$d_{\text{cal}}$ (Å)	$hkl$	$d_{\text{cal}}$ (Å)	$hkl$
5.40 <sup>c</sup>	0.2			3.46	1			3.46	300
3.21	20	3.21	021	3.18	15	3.18	021		
				3.09	2			3.09	0012
				3.03	5			3.02	306
2.93	2	2.93	002	2.86	1.5	2.86	002		
2.71	6	2.71	220	2.71	4	2.71	220		
2.23	0.2	2.23	212						
				2.31	1.5			2.31	3012
2.12	0.3	2.10	230					2.00	330
				2.01	2				
1.99	5	1.99	222	1.97	4	1.97	222		
1.92	3	1.92	040	1.92	2.5	1.92	040		

Note. Specimen A, quenched from 800°C in water; specimen B, quenched and successively reheated at 400°C for 72 hr.

<sup>a</sup>  $a = 7.68$  and  $c = 5.86$  Å.

<sup>b</sup>  $a = 7.68$  and  $c = 5.72$  Å.

<sup>c</sup> Due to incommensurate superstructure.

ential thermal analysis (DTA) was performed in air with the heating or cooling rate of 10°C/min (Rigaku TG-DTA high-temperature type).

### 3. Experimental Results

#### 3.1. Phase Relation

The phase of the quenched specimen (specimen A in Table I) was analyzed by means of X-ray powder diffraction and most of the strong reflections could be indexed on the basis of the  $\beta$ -phase ( $a = 7.68$  and  $c = 5.86$  Å). A weak reflection indicates the formation of the superstructure, which will be discussed in Section 3.2. Specimen B, when reheated at 400°C for 72 hr, gave reflections not only from the  $\beta$ -phase but also from another phase. The latter is considered to be due to the formation of a second phase which is stable only at

low temperatures. On reheating, the  $c$  value of the matrix  $\beta$ -phase changes remarkably, from 5.86 to 5.72 Å, while the  $a$  value is almost unchanged. A similar change is observed for the specimen reheated at 250°C.

On DTA measurement of the reheated specimen a clear endothermic peak appeared at about 595°C in the course of heating. This must be due to the transition of the second phase to the  $\beta$ -phase. In the course of cooling the opposite transition occurred at about 590°C.

Fig. 1a is a microscope image of the quenched specimen. The pattern of the microscope image is composed of ill-defined bands, running normal to the  $c$  direction. This is always the case for the quenched specimen when the electron beam is incident normal to the  $c$  direction. The contrast must be mainly due to the lattice strain, which is essentially related to the formation of the superstructure mentioned later.

The specimen is sensitive to irradiation by the electron beam. In order to avoid the irradiation damage, direct magnification was limited to less than  $5 \times 10^4$  times at maximum. Once the density of electrons is increased in order to get higher magnification, the image pattern quickly changes, as shown in Fig. 1b. It became much more complex, but locally there arise simple arrays of bright and dark dots. Such a simple array at the area marked by arrows can be interpreted based on the reported structure of  $\beta$ -phase (2); i.e., the dark dots represent the sites of cations projected in one of the  $a$  directions. The observation suggests that the structure in the quenched specimen is essentially the same as that of the  $\beta$ -phase, being consistent with the result by the X-ray diffraction above.

Electron diffraction patterns were taken from the second phase, which appeared on reheating, tilting the specimen in the microscope. Two patterns are presented in Figs. 2a and 2b. It may be seen that the crystal exhibits rhombohedral symmetry with lat-

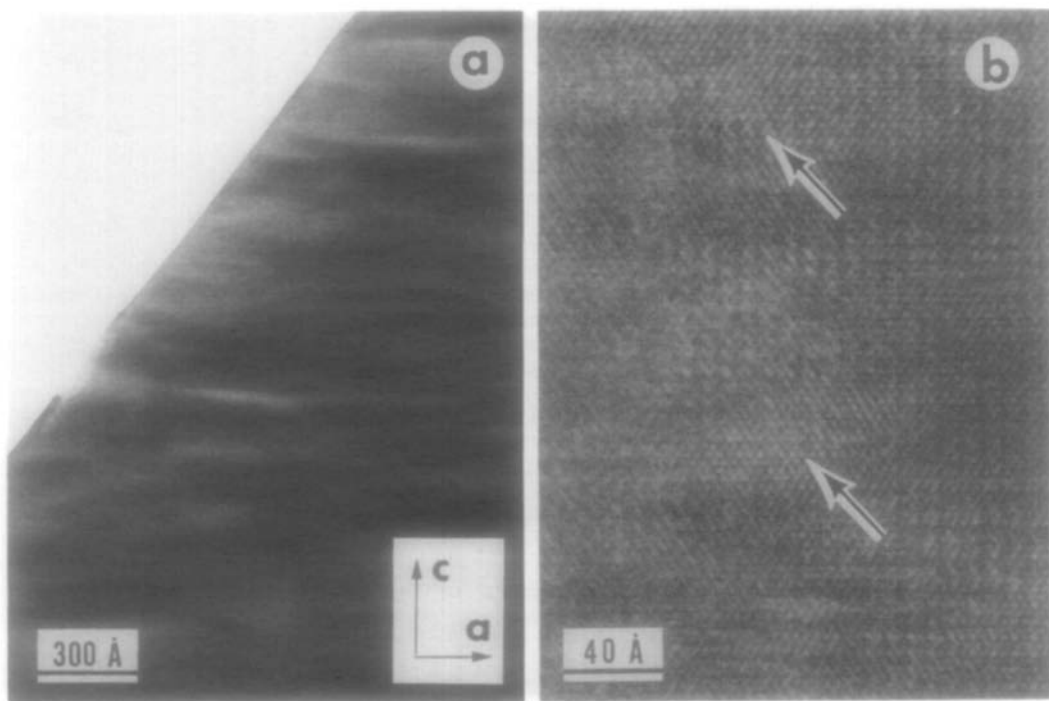


FIG. 1. (a) Electron micrograph of the specimen quenched from 800°C. (b) After the strong electron irradiation of the same specimen, the array of dots at the areas marked by arrows can be interpreted simply by the  $\beta$ -phase without any superstructure.

tice parameters  $a = 12.0$  and  $c = 37.1$  Å in the hexagonal representation. Figure 2c shows a micrograph of the second phase. There is no prominent pattern except hexagonal ones due to the surface steps, which must have been formed by cleavage.

The  $\beta$ -phase, having remained in the reheated specimen, does not vary the apparent microstructure in spite of the remarkable change in the lattice parameters; i.e., it still exhibits the ill-defined bands.

### 3.2. Superstructures

Electron diffraction patterns taken from the quenched specimen are shown in Fig. 3a with the electron beam incident along the  $hhl$  zone axis. In addition to the reflections that can be indexed on the basis of the  $\beta$ -phase, extra ones appear along the  $c^*$  direction. The latter locate at nonintegral po-

sitions and this indicates formation of a superstructure of the incommensurate type. We may ascribe it to the formation of a one-dimensional modulated structure, which can be described based on a four-dimensional space (3, 4). If we write the fundamental reflections of the conventional  $\beta$ -phase in the reciprocal lattice by  $h_1a^* + h_2b^* + h_3c^* = h$ , extra reflections are denoted by  $h + h_4k$ , where  $h_1, h_2, h_3, h_4$  are integers.  $k$  is related to the modulated structure by  $k = \alpha c^*$ , where  $1/|k|$  means the wave length. In the present case  $\alpha$  is measured to be  $0.34 \pm 0.01$ . Figure 3b shows the index of each reflection in Fig. 3a by means of  $h_1h_2h_3h_4$ . Very weak satellite reflections may be due to double reflection.

When the specimen is tilted in the microscope, the superstructure reflections change the array in diffraction patterns.

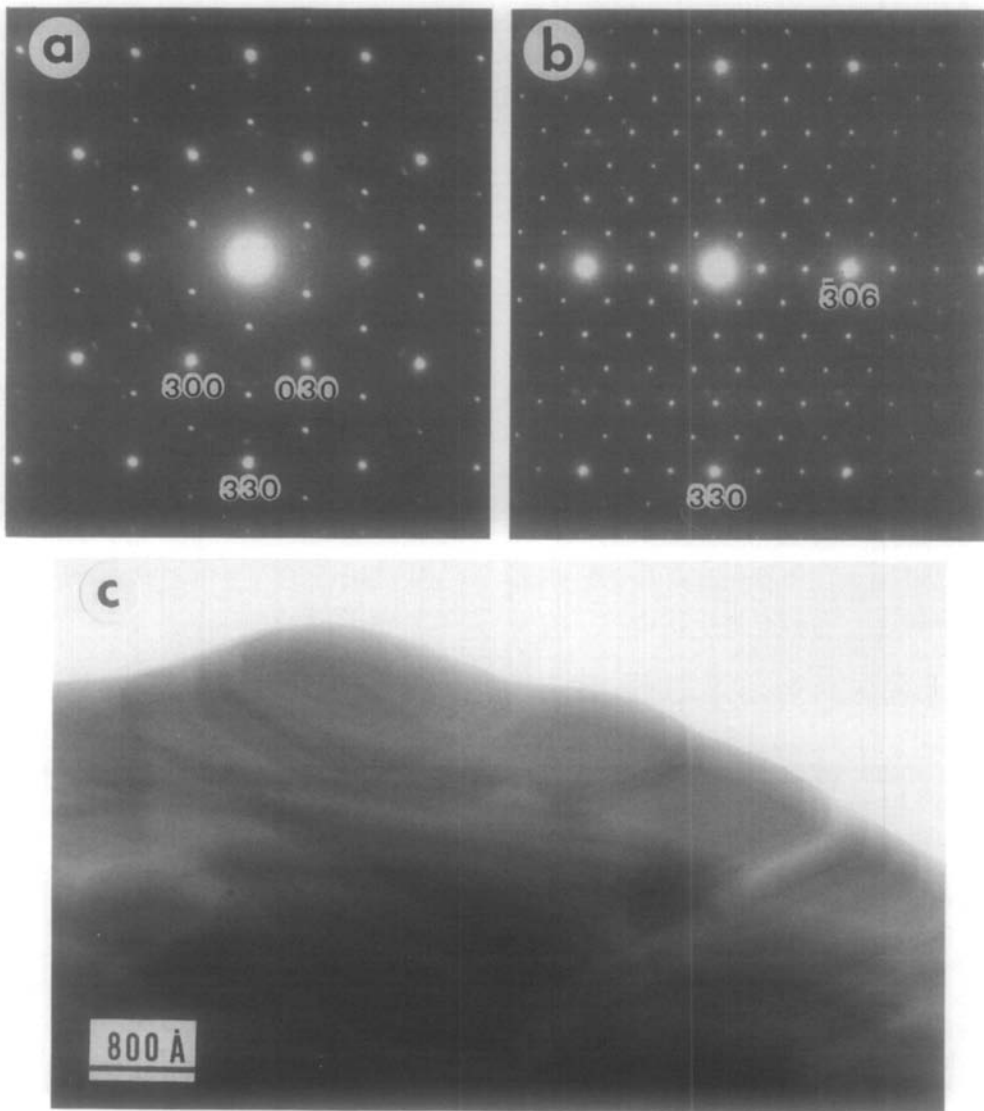


FIG. 2. Electron diffraction patterns taken from the second phase (rhombohedral,  $a = 12.0$  and  $c = 37.1$  Å) formed on reheating. (a) Electron beam is incident along the  $hk0$  zone axis. (b) Taken after tilting about  $30^\circ$  around the  $330$  axis. (c) A micrograph in which there are hexagonal patterns due to cleavage.

However, they can be indexed with the same value of  $\alpha$ .

The residual matrix of the  $\beta$ -phase in the reheated specimens gave the diffraction patterns as in Fig. 3c. It is similar to Fig. 3a but the positions of extra reflections are slightly different. The value of  $\alpha$  is mea-

sured to be  $0.37 \pm 0.01$  for specimens reheated at 400 or 250°C.

### 3.3. Precipitation of the Second Phase

A possible explanation for the change in the lattice parameters of the  $\beta$ -phase on reheating is due to the variation in the chemi-

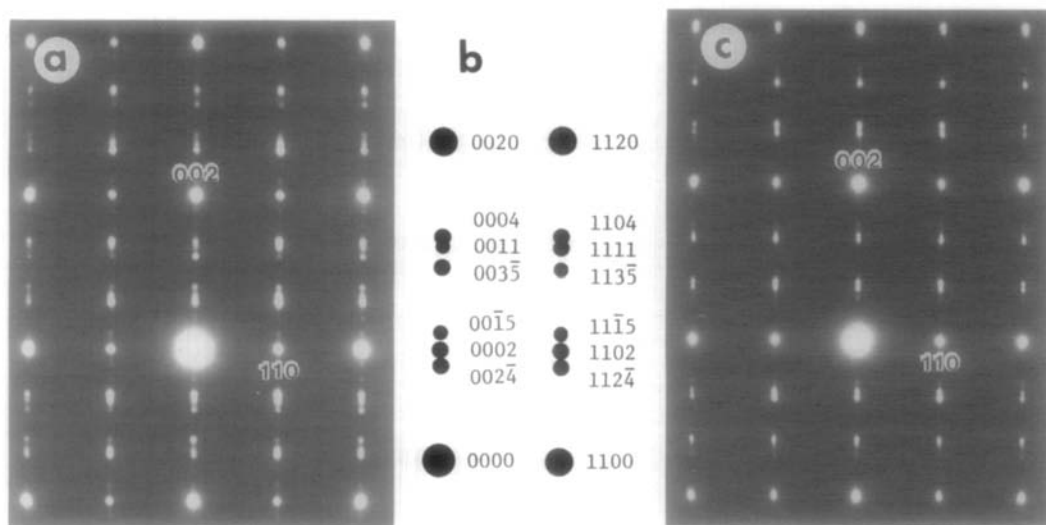


FIG. 3. Electron diffraction patterns taken from the  $\beta$ -phase with a modulated structure, after being quenched from 800°C (a) and successively reheated at 400°C (c). (b) The index of (a) based on an incommensurate superstructure.

cal composition. From this standpoint a series of specimens were prepared at 800°C with different composition ratios of Bi<sub>2</sub>O<sub>3</sub> and PbF<sub>2</sub>, followed by quenching in water. The  $\beta$ -phase obtained with the starting composition 95% Bi<sub>2</sub>O<sub>3</sub>·5% PbF<sub>2</sub> has similar lattice parameters to those of the reheated specimen mentioned above.

No phase diagram has been proposed for Bi<sub>2</sub>O<sub>3</sub>-PbF<sub>2</sub>. The large variation in the chemical composition would suggest that the occurrence of the second phase is due to phase decomposition. This implies that PbF<sub>2</sub> is richer in the second phase, which appears only at lower temperature range, than in the residual  $\beta$ -phase.

When a specimen is slowly cooled from 800°C, the second phase always appears together with the residual  $\beta$ -phase. This may be explained by the occurrence of the phase decomposition mentioned above.

Although local, small precipitates elongating in the  $c$  direction are observed in the residual  $\beta$ -phase of reheated specimens (Fig. 4a). When the intensity of the electron

beam becomes stronger, structural changes occur as shown in Figs. 4b and 4c. In Fig. 4b the precipitates become slightly clear. In Fig. 4c new grains appear, while the elongated precipitates disappear. The diffraction patterns from them do not coincide with those from the second phase mentioned above (Figs. 2a and 2b). The sequential observation however suggests that the precipitates are metastable and formed only prior to the stable phase.

In order to observe the precipitates more clearly, an additional heat treatment was done; i.e., the reheated specimen was further heated at 700°C for 24 hr and quenched in water. This additional process produced the  $\beta$ -phase without the ill-defined bands structure. The specimen was then heated either at 400 or 250°C. Figure 5a shows a micrograph of the specimen heated at 400°C for 72 hr. Rod-like precipitates appear with the elongation along the  $c$  direction.

Figure 5b is a high-magnification lattice image of the  $\beta$ -phase matrix, in which rod-like precipitates are included. No extra pat-

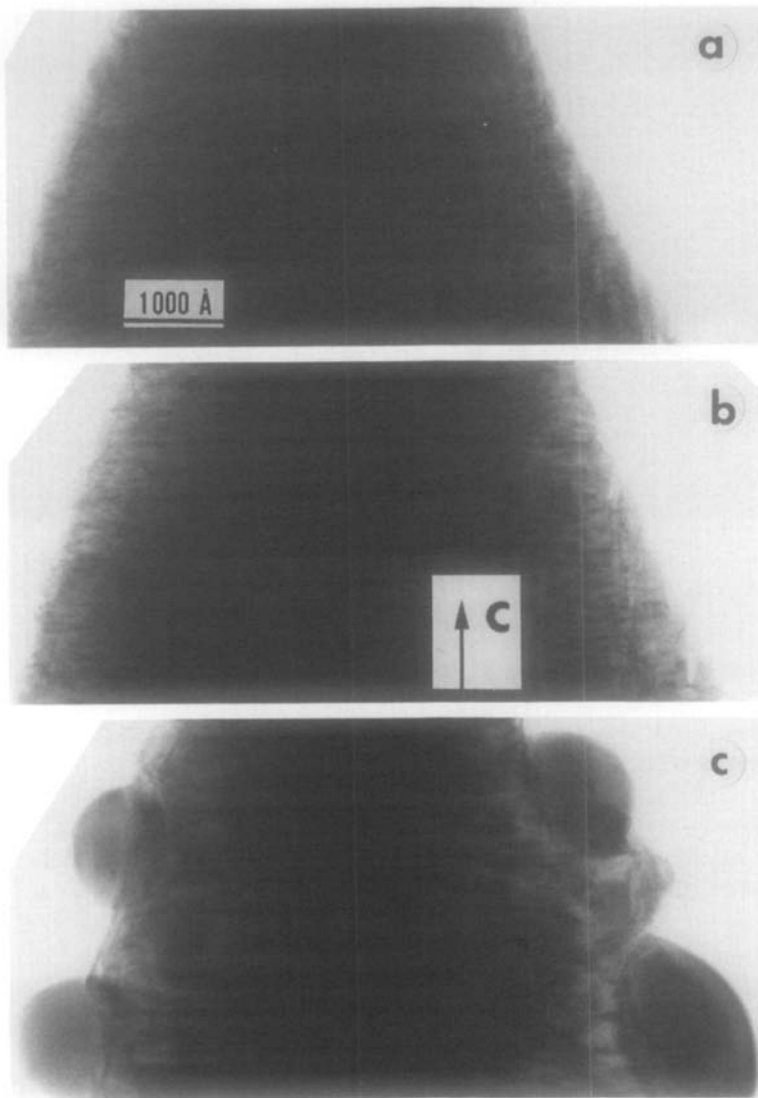


FIG. 4. Structural variation in the  $\beta$ -phase matrix under strong electron irradiation. (a) An initial state, (b) sharpening in the contrast of precipitates, and (c) formation of small grains.

tern is found inside the precipitates except a weak Moiré pattern. This means that nothing but lattice spacings change between the matrix and the precipitates. The small change in the lattice spacing may be related to that in the chemical composition. The image contrast of the matrix is essentially similar to what is expected from the known

structure (2). At the parts marked by arrows, electron damage has occurred. Detailed analysis on the structure of the  $\beta$ -phase will be given elsewhere.

The shape of the precipitates depends on the reheating temperature. Figure 6 shows the micrograph of the precipitation that occurred at 250°C for 120 hr, with the electron

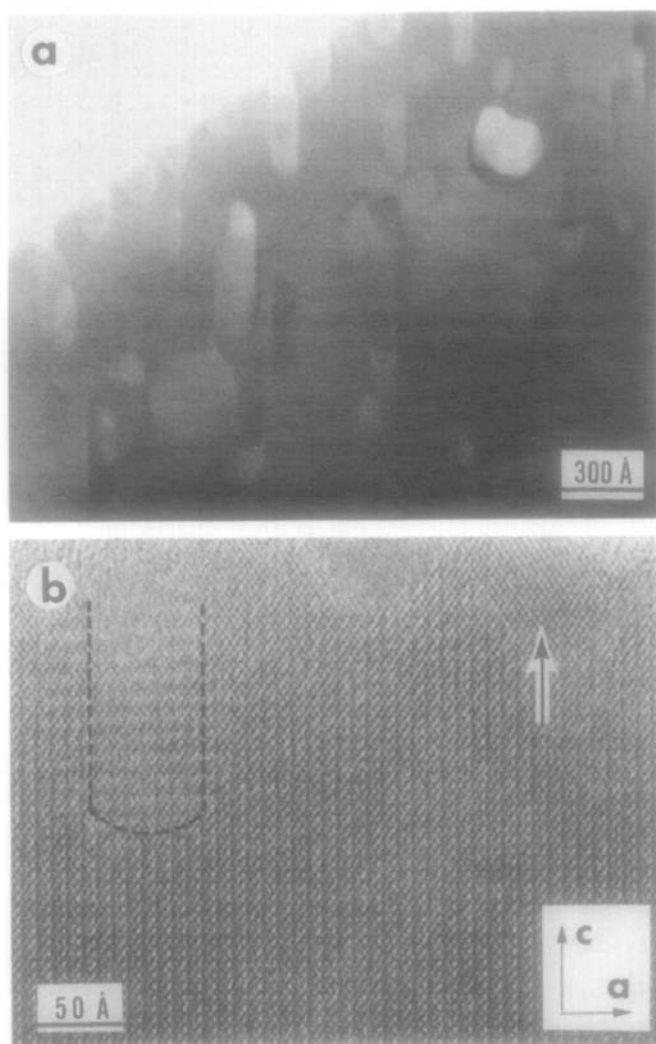


FIG. 5. (a) Elongated precipitates appearing on reheating at 400°C. (b) High-magnification image of the  $\beta$ -phase matrix including a precipitate, outlined by dotted lines.

beam almost parallel to the  $hhl$  zone axis. It occurs along the  $\{110\}$  plane, being parallel to the incident electron beam. It is interesting to note that most of the habit planes are formed in pairs. The contrast of lattice fringe images is similar to that of the GP zones in Al-Cu alloys (5), suggesting that they are due to the strain, which has originated from the segregation of foreign atoms, Pb or/and F. The interaction between

the strain fields of neighboring habit planes is presumably so strong that they are formed in pairs. In the diffraction pattern weak streaks are observed along the  $\langle 110 \rangle$  directions, i.e., normal to the habit planes.

#### 4. Discussion

It is known (6) that the  $\beta$ -phase is stabilized by the addition of 4–10% Sb<sub>2</sub>O<sub>3</sub> into

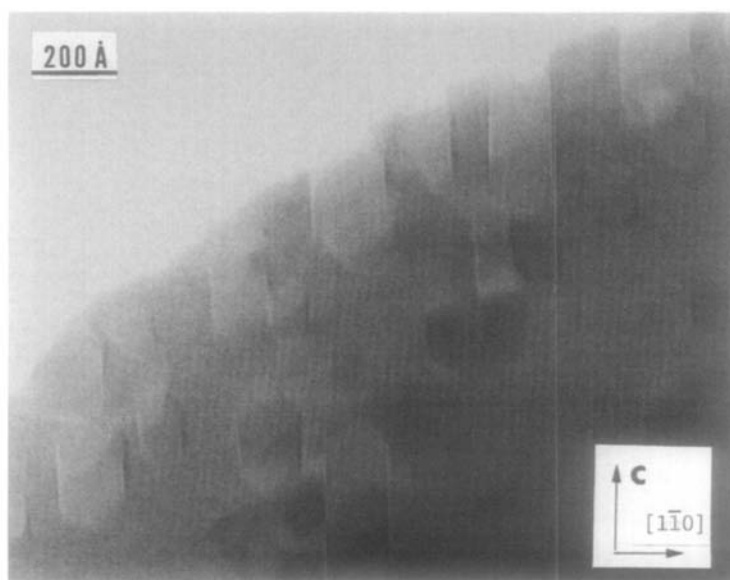


FIG. 6. GP zone-like precipitation occurring at 250°C.

$\text{Bi}_2\text{O}_3$  and that more than 50% of  $\text{Sb}^{3+}$  changes to  $\text{Sb}^{5+}$  in the crystal. There are open spaces in the structure of the  $\beta$ -phase (2), making tunnels along the  $c$  direction. The existence of the  $\text{Sb}^{5+}$  means the occurrence of excess oxide ions, which are probably accommodated in the tunnel-like space, from the viewpoint of charge neutrality. The invasion of oxide ions suppresses the phase transition of  $\beta$  to  $\alpha$ . In other words, it makes the stability of the  $\beta$ -phase higher. In the present case, a small amount of oxide or fluoride ions become excess from the viewpoint of composition. They are also considered to be accommodated in the tunnel-like spaces in the structure of the  $\beta$ -phase. The transition to the  $\alpha$ -phase is suppressed and, as a result, the  $\beta$ -phase is stabilized at room temperature.

The regular arrangement of excess oxide or fluoride ions must be related to the formation of the superstructure and, at the same time, produces the ill-defined bands of the  $\beta$ -phase (Fig. 1a). When the  $\beta$ -phase is irradiated by a strong electron beam, the

interstitial oxide or fluoride ions are easily shifted or knocked-out and, as a result, the structure becomes simple without any superlattice, at least locally.

The wavelength of the structure modulation is expressed by  $1/|k| = c/\alpha$ . The value is very much smaller than the apparent separation of the ill-defined bands, which is between 100 and 300 Å. This means that the image contrast in Fig. 1a does not reflect directly the modulation of the structure. A possible explanation for this observation is that the crystal in Fig. 1a has suffered from slight damage due to electron irradiation, which was necessary for taking the photograph. The image contrast of ill-defined bands must be ascribed mainly to the local fluctuation of the strain, which was generated by the small amount of irradiation.

#### Acknowledgments

The authors express their deep gratitude to Dr. A. Yamamoto for his discussion and Messrs. Y. Kitami, M. Yokoyama, and Y. Yajima for the experimental support.



**References**

1. S. HORIUCHI AND K. UCHIDA, *J. Am. Ceram. Soc.* **68**, C-220 (1985).
2. B. AURIVILLIUS AND G. MALMROS, *Trans. R. Inst. Technol. Stockholm* **291**, 545 (1972).
3. P. M. DEWOLF, T. JANSSEN, AND A. JANNER, *Acta Crystallogr. Sect. A* **37**, 625 (1981).
4. A. YAMAMOTO AND H. NAKAZAWA, *Acta Crystallogr. Sect. A* **38**, 79 (1982).
5. T. SATO, Y. KOJIMA, AND T. TAKAHASHI, *Trans. Japan. Inst. Metals* **6**, 386 (1983).
6. M. MIYAYAMA, H. TERADA, AND H. YANAGIDA, *J. Amer. Ceram. Soc.* **64**, C-19 (1981).